

# Excitations of N<sub>2</sub> and O<sub>2</sub> molecules due to helium ion impact and a polarization effect

M. Gochitashvili<sup>1</sup>, R. Lomsadze<sup>1</sup>, R. Ya. Kezerashvili<sup>2,3</sup>, I. Noselidze<sup>1</sup>, and M. Schulz<sup>4</sup>

<sup>1</sup>*Tbilisi State University, 0179 Tbilisi, Georgia*

<sup>2</sup>*New York City College of Technology,  
The City University of New York,  
Brooklyn, NY 11201, USA*

<sup>3</sup>*The Graduate School and University Center,  
The City University of New York,  
New York, NY 10016, USA*

<sup>4</sup>*Missouri University of Science and Technology,  
Rolla, MO 65409, USA*

(Dated: January 30, 2024)

We present an experimental study of the dissociative excitation in the collision of helium ions with nitrogen and oxygen molecules for collision energy of 0.7 – 10 keV. Absolute emission cross sections are measured and reported for most nitrogen and oxygen atomic and ionic lines in wide, vacuum ultraviolet (80 – 130 nm) and visible (380 – 800 nm), spectral regions. Remarkable similarities of the processes realized in He<sup>+</sup>+N<sub>2</sub> and He<sup>+</sup>+O<sub>2</sub> collision systems are observed. We present polarization measurements for He<sup>+</sup>+N<sub>2</sub> collision system.

The emission of excited dissociative products was detected using an improved high-resolution optical spectroscopy method. This method incorporates the retarding potential method and a high resolution electrostatic energy analyzer to precisely measure the energy of incident particles and the energy of dispersion. The improvement in the optics resolution allows us to measure the cross section on the order of 10<sup>-19</sup> cm<sup>2</sup> or lower.

## I. INTRODUCTION

Nitrogen and oxygen molecules are the main constituents of the atmosphere and are simple species of great interest for interstellar medium [1–4]. First, all nitrogen and oxygen molecules are important constituents of the upper atmosphere of planets and play a crucial role in atmospheric chemistry at mesospheric and thermosphere altitudes. Solar radiation mainly results from solar flares, solar wind, coronal mass ejections, and solar prominences and includes electromagnetic radiation and energetic electrons, protons, and  $\alpha$ -particles. These basic components of solar radiation interact with atmospheric nitrogen and oxygen molecules: electromagnetic radiation with energies from a few tenths of eV to hundreds of MeV, electrons and protons in the energy spectrum from a few tenths of eV to hundreds of MeV and up to GeV, and helium ions with energies up to 10 keV. Numerous processes of the formation of atoms or atomic ions in which oxygen and nitrogen molecules act as targets, have attracted considerable interest. These processes play a crucial role in atmospheric chemistry at mesospheric and thermosphere altitudes. Ionic species are present in the upper atmosphere of planets and govern ionosphere chemistry. Atomic and molecular ions have also been detected in the comet tails. Among the many inelastic processes involving oxygen ions, excitation, ionization, and charge exchange are relevant to the low-temperature edge plasma region of current thermonuclear fusion devices [5, 6]. Oxygen is also typical impurity in almost all laboratory plasmas [5].

The electromagnetic radiation, the corpuscular part of the solar radiation, that is electrons, protons, and helium ions [7] with an energy spectrum between a few tenths of eV and hundreds of MeV, are heading towards the Earth, and interact with the atmosphere. The corpuscular part of solar radiation is deflected by the Earth's magnetic field towards the poles and is scattered and absorbed by atmospheric atoms and molecules, particularly by nitrogen and oxygen. The accompanying ionization of various gases in the upper atmosphere causes a luminous glow in the upper atmosphere, the so-called phenomenon of - aurora. Although there have been investigations of the main characteristics of the aurora, there is still a lack of quantitative description of this phenomenon. Upon reaching the denser layers of the atmosphere, electrons and helium ions participate in various inelastic processes such as ionization, molecular excitation, and charge-exchange reactions on atmospheric gases, especially nitrogen and oxygen molecules. Spectral analysis of the aurora shows that ionized nitrogen molecules can radiate in the visible, infrared, and ultraviolet region.

Observations of the excitation of B <sup>2</sup> $\Sigma_u^+$  and A <sup>2</sup> $\Pi_u$  band systems in the ionized nitrogen molecule N<sub>2</sub><sup>+</sup> indicate their presence in the aurora and dayglow [8–13]. These bands appear in the spectra of polar auroras and contain information on the collision processes in the upper atmosphere. Hence, during collisions, vibrationally excited N<sub>2</sub><sup>+</sup> ions and their radiative decay are accompanied by the creation of electronic ground X <sup>2</sup> $\Sigma_g^+$  states.

The study of emission spectra provides an opportunity to determine the concentration and energy distribution of particles entering the upper layer of the atmosphere. To address this problem, it is necessary to determine high-precision absolute cross-sections of various inelastic processes, such as ionization, excitation, and charge-exchange.

However, the determination of the absolute cross-section, for example, of the excited B  $^2\Sigma_u^+$  band system is challenging. The number of experimental studies in which this excited band system is measured is very limited, and these studies are usually related to the processes of excitation through electron collisions with nitrogen molecules [14–18]. However, in the case of electron impact, the experimentally determined cross-section for the formation of  $N_2^+$  ions in the A–state is only known to be within 50% because measurements of excitation cross-sections involve various challenges. In particular, the lifetime of nitrogen molecule ions in the A  $^2\Pi_u$  state is approximately  $10^{-5}$  s [14, 15], and during measurements the quenching of excited particles (the transfer of the excited energy to other particles) is expected to occur.

The dissociation of highly excited molecular states deserves special interest and is the subject of extensive research [19–28], including experimental investigations that add new information. The products of the molecular dissociation may remain in an excited state. Highly excited states may decay through pre-dissociation or autoionization channels with the formation of a neutral atom, electron, or ion [20–22, 24]. For example, neutral fragments resulting from the dissociation of highly excited states were reported in Refs. [23, 25–28]. The absolute cross-section of the luminescence due to the excited product of atomic oxygen dissociation in the wavelength range of 97–131 nm was measured for photoionization [29].

Polarization information is important for the accurate determination of absolute and relative photon emission cross-sections. The results of the polarization measurements also allowed some nontrivial conclusions related to the spatial distribution of the electron cloud. A reliable experimental determination of the polarization fraction, not only provides additional information about the details of excitation cross-sections by determining the relative populations of the degenerate magnetic sublevels, but also enables a comparison of available experimental data with calculations of total cross-sections.

Quantitatively, the polarization fraction can be analyzed in terms of the alignment of orbital momentum sublevels. The cross-sections of the population of magnetic sublevels provide detailed information on the excitation mechanism. Owing to the different populations of magnetic sublevels within a certain ( $nl$ ) subshell, the radiation can be polarized and, consequently, anisotropic.

Numerous studies have investigated the polarization of radiation in ion-atom and ion-molecule processes [30–42]. Usually, in polarization measurements, coincidences of the photon and scattered particle are detected [33–38].

In the case of inelastic  $He^+ - N_2$  and  $He^+ - O_2$  collisions, the radiation spectrum is multitudinous. Therefore, a monochromator with a high resolving power ( $\sim 0.2$  nm) should be used. To amplify the optical registration sensitivity in addition to the monochromator, broad bandpass filters were used for isolating the optical lines. An anisotropic excitation mechanism is common in astrophysical plasmas and is readily reproduced in a laboratory environment [43]. Almost a century ago [44], it was shown that spectral line emissions originating from atoms or ions excited by particles whose velocity distribution is anisotropic, in general, are polarized. If collisional excitation occurs by impact in a preferred direction, the magnetic sublevels of the excited states can be populated with non-statistical probabilities. When the state decays, the emitted electromagnetic radiation becomes spatially anisotropic and partially polarized [45].

In Ref. [46], the authors studied the polarization of the radiation emitted from ions excited by an electron beam impact inside an electron-beam ion trap. This demonstrates that the polarization of the emitted radiation is especially important when measurements are made with spectrometers in which the energy disperser is polarization-selective. Polarization-sensitive measurements may also be used to detect resonance processes that are too weak to be directly observed. Moreover, this provides information about the magnetic sublevels that would normally remain hidden in simple energy dispersive measurements.

Applying conservation of angular momentum allows the calculation of the relative populations of the magnetic sublevels [47]. The magnetic sublevel population of the autoionizing states of helium, excited by the charged particle impact was determined in Refs. [48, 49]. The degree of polarization of the radiation emitted by atoms and ions following particle impact contains information on the excitation of magnetic sublevels with different projections  $M$  of orbital momentum [50]. In Ref. [48], the authors measured the degree of linear polarization in the extreme ultraviolet region and cross-sections of excitation to individual magnetic sublevels. For the 1s-2p single-electron excitation of helium, it was found that the effects are stronger for the excitation of sublevels with  $M = 0$ , than with  $M = \pm 1$ . In the literature, considerable evidence exists that molecular radiation may be strongly polarized for both discharge sources and when electron beam excitation is used [51]. In Ref. [52], the authors predicted that atomic or ionic radiation following dissociative excitation of molecules can be polarized. Several excited states of the N and  $N^+$  were identified in the visible and near-infrared optical emission spectra produced by the electron impact excitation of the  $N_2$  ( $X^1\Sigma_g^+$ ) [53]. During the dissociation process, one of the fragments (ion/atom) can be left in an excited state from which it radiates. The fluorescence from the excited atomic fragment can be polarized, and the degree of this polarization is related to the form of anisotropy in the angular distribution of the dissociation product [54].

In the last few years, experimental studies on ion collisions at low and medium energies (a few eV and keV) have been performed using different techniques. For example, in the case of the interaction between  $He^+$  ions and  $H_2$ ,  $N_2$ ,

$O_2$ ,  $CO$ , and  $NO$  molecules, collision spectroscopy methods [55–57], and high resolution translational spectroscopy for the pairs  $H_2^+ - H_2$ ,  $H_2^+ - Mg$ ,  $H_2^+ - Na$ ,  $H_2^+ - Cs$ , and  $H_2^+ - Ar$  [58] have been used. Emission from the dissociation products in the visible range revealed a rich spectrum of excited states in the collisions of different ions with  $O_2$  and  $N_2$  molecules [59, 60].

In this work, we experimentally studied dissociative excitation in collisions of helium ions with nitrogen and oxygen molecules in the ion energy range of 0.7–10 keV. One of the reasons for the choice of the helium ion as a projectile is that highly excited molecular states of the oxygen and nitrogen molecular ion arise in this case because the inelastic channels of charge exchange prevail in the respective range of collision energies, and thus the inner-shell electrons of the molecules are captured [55, 61]. Absolute emission cross-sections were measured and reported for most nitrogen and oxygen atomic and ionic lines in the vacuum ultraviolet (80–130 nm) and visible (380–800 nm), spectral regions. The measurements were performed using high-resolution optical spectroscopy [62, 63]. We report the measurements of the degree of linear polarization for the lines of the helium atom  $\lambda = 388.9$  nm for the transition  $3p\ ^3P_0 \rightarrow 2s\ ^3S$  and  $\lambda = 587.6$  nm, the transition  $3d\ ^3D \rightarrow 2p\ ^3P$  and nitrogen ion  $\lambda = 500.1 - 500.5$  nm, the transition  $3d\ ^3F_0 \rightarrow 3p\ ^3D$  due to the  $He^+ - N_2$  collision.

The remainder of this paper is organized as follows. In Sec. II, we present the experimental setup and measurement method. In Sec. III, we present the processes and emission spectral lines measured for the  $He^+ - N_2$  and  $He^+ - O_2$  collision systems, and discuss the results of the measurements. Finally, conclusions follow in Sec. IV.

## II. EXPERIMENT SETUP AND MEASUREMENT METHOD

The radiation from the excited particles was detected using high-resolution optical spectroscopy, which is the most precise method for the identification of highly excited molecular states. The experimental setup and calibration procedure are described in detail in Refs. [62, 63]. The resolution of the optics has greatly improved since then; therefore, we were able to distinguish the excitation channels and measure the cross-section on the order of  $10^{-19}$  cm<sup>2</sup> or lower.

A schematic of the experimental setup is shown in Fig. 1. A beam of  $He^+$  ions extracted from the high-frequency (20 MHz) discharge ion source is accelerated, collimated, and focused by an ion-optics system, which includes quadrupole lenses and collimating slits, and mass-selected with a  $60^\circ$  magnetic sector field. The beam was then directed into the collision chamber. We used an electron gun placed in the mass-analyzer chamber to determine the spectral sensitivity of the emission detection system. After the collimation and additional focusing, the electron beam is directed into the collision chamber.

The radiation emitted as a result of the excitation of colliding particles was observed at  $90^\circ$  with respect to the direction of the ion beam. A secondary-electron multiplier with a cooled cathode in both integral and counting regimes detects the radiation. The spectroscopic analysis of the emission is performed by a visible monochromator

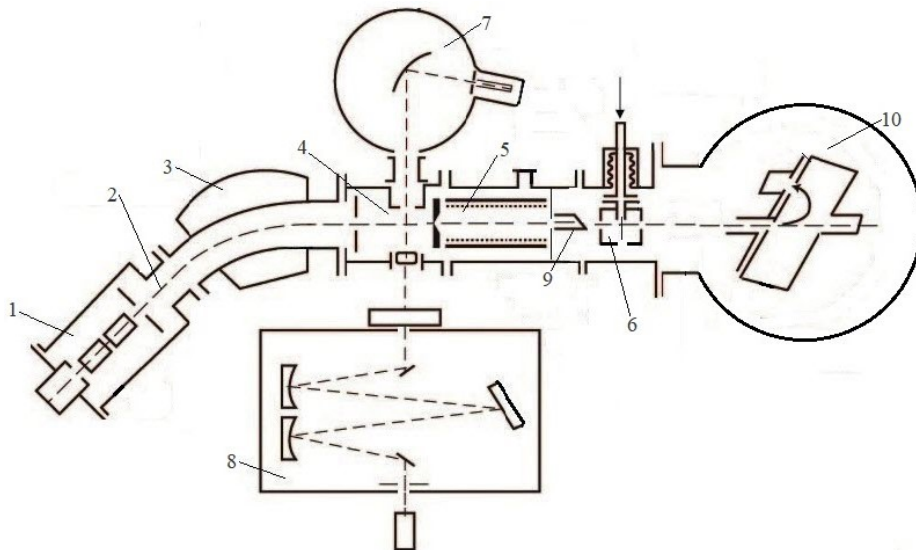


FIG. 1: (Color online) Schematic diagram of the experimental set up: 1 - ion source, 2 - ion beam, 3 - magnet mass-analyzer, 4 - first collision chamber, 5 - second collision chamber, 6 - third collision chamber, 7 - vacuum ultraviolet spectrometer, 8 - visible spectrometer, 9 - Faraday cup, 10 - electrostatic analyzer.

with resolution of 40 nm/mm, and by means of a Seya–Namioka vacuum monochromator with a toroidal diffraction grating with a typical resolution of 0.05 nm that has a 1200 line/mm. The method also allowed us to measure the polarization of excitation, which itself is a powerful tool for establishing the mechanism for inelastic processes. A polarizer and a mica quarter-wave phase plate are placed in front of the entrance slit of the monochromator and the linear polarization of the emission is analyzed. For cancellation of the polarizing effect of the monochromator, the phase plate are placed after the polarizer and rigidly coupled to it.

The measurements at low-energy collisions required precise determination of the energy of helium ions as well as their energy dispersion. To avoid errors in the measurements of the energy of the incident particles, we employed the retarding potential method and used an electrostatic analyzer with a resolving power of 700. Additionally, by measuring the energy of the impacting particles, we estimate the dispersion of energy provided by the high-frequency ion source and electron gun.

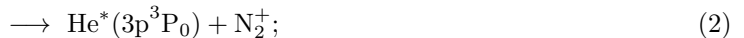
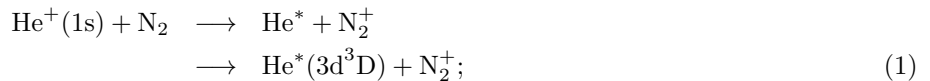
The helium ion current in the collision chamber was on the order 0.1–0.5  $\mu\text{A}$ , while the electron current was 5–20  $\mu\text{A}$ . The pressure of the target gas under investigation did not exceed  $6 \times 10^{-4}$  Torr; therefore, single collisions were considered. The system was differentially pumped using an oil-free diffusion pump. The residual gas pressure did not exceed  $0.1 \times 10^{-6}$  Torr.

The basic problem in finding the cross-section is determining the relative and absolute spectral sensitivities of the radiation-detecting system. This was achieved by measuring the output signal of the photomultiplier owing to the (0.0), (0.1), (0.2), (0.3), (0.4), (1.2), (1.3), and (1.4) bands in the first negative system of the ion  $\text{N}_2^+$  ( $\text{B } ^2\Sigma_u^+ - \text{X } ^2\Sigma_g^+$  transition) and (4.0), (4.1), (6.2), (6.3), (2.0), (3.0), (5.1), and (5.2) bands of the Meinel system ( $\text{A } ^2\Pi_u^+ - \text{X } ^2\Sigma_g^+$  transition) [62] excited in collisions between the electrons ( $E_e = 110$  eV) and nitrogen molecules. The output signal was normalized to the (0.1) band with the corresponding wavelength  $\lambda = 427.8$  nm. This line has high intensity in this range. The relative spectral sensitivity of the recording system obtained in this manner was compared with the relative excitation cross-sections for the same bands, averaged over the experimental data reported in Refs. [64–67]. The absolute excitation cross-sections for the (0.1) band ( $\lambda = 427.8$  nm) were assumed to be  $5.3 \times 10^{-18}$   $\text{cm}^2$  at an electron energy of 110 eV. This value was taken from Ref. [11]. The relative and absolute uncertainties in our measurements were 5% and 15%, respectively. The accuracy of the polarization measurements did not exceed  $\sim 2$  %.

### III. RESULTS OF EXPERIMENTAL MEASUREMENTS AND DISCUSSION

Sub-sections III A and III B provide an outline of the investigated processes for the  $\text{He}^+ - \text{N}_2$  and  $\text{He}^+ - \text{O}_2$  collision systems and emission spectral lines. In Sub-sections III C and III D, we present the experimental results and their discussion.

#### A. $\text{He}^+ - \text{N}_2$ collision system



and



when

$$\begin{aligned} \text{N}_2^{+**} &\longrightarrow \text{N}^*(2p^4 \ ^4\text{P}) + \text{N}^+(1s^2 2s^2 2p^2 \ ^3\text{P}); \\ &\longrightarrow \text{N}^*(3s4\text{P}) + \text{N}^+(2p^2 \ ^3\text{P}); \end{aligned} \quad (6)$$

$$\longrightarrow \text{N}^*(3s' \ ^2\text{D}) + \text{N}^+(2p^2 \ ^3\text{P}); \quad (7)$$

$$\longrightarrow \text{N}^*(4p^2\text{S}^0) + \text{N}^+(2p^2 \ ^3\text{P}); \quad (8)$$

$$\longrightarrow \text{N}(1s^2 2s^2 2p^3 \ ^4\text{S}_{3/2}^0) + \text{N}^{+*}(1s^2 2s^2 2p^1 3p \ ^1\text{P}); \quad (9)$$

$$\longrightarrow \text{N}(1s^2 2s^2 2p^3 \ ^4\text{S}_{3/2}^0) + \text{N}^{+*}(3p \ ^3\text{D}); \quad (10)$$

$$\longrightarrow \text{N}(1s^2 2s^2 2p^3 \ ^4\text{S}_{3/2}^0) + \text{N}^{+*}(3d \ ^3\text{F}^0); \quad (11)$$

$$\longrightarrow \text{N}(1s^2 2s^2 2p^3 \ ^4\text{S}_{3/2}^0) + \text{N}^{+*}(3s \ ^3\text{P}^0); \quad (12)$$

$$\longrightarrow \text{N}(1s^2 2s^2 2p^3 \ ^4\text{S}_{3/2}^0) + \text{N}^{+*}(4f \ \text{F}); \quad (13)$$

$$\longrightarrow \text{N}(1s^2 2s^2 2p^3 \ ^4\text{S}_{3/2}^0) + \text{N}^{+*}(2p^3 \ ^3\text{D}^0). \quad (14)$$

The nitrogen atom and ion lines wavelength and corresponding transitions are the following

Nitrogen atom			Nitrogen ion		
	Wavelength, $\lambda$ nm	Transition		Wavelength, $\lambda$ nm	Transition
NI	493.5	$4p \ ^2\text{S}^0 \longrightarrow 3s \ ^2\text{P}$	NII	648.2	$3p \ ^1\text{P} \longrightarrow 3s \ ^1\text{P}^0$
NI	124.3	$3s' \ ^3\text{D} \longrightarrow 2p^3 \ ^4\text{D}^0$	NII	504.5	$3p \ ^3\text{S} \longrightarrow 3s \ ^3\text{P}^0$
NI	120	$3s \ ^4\text{P} \longrightarrow 2p^3 \ ^4\text{S}^0$	NII	500.5	$3d \ ^3\text{F}^0 \longrightarrow 3p \ ^3\text{D}$
NI	113.4–113.5	$2p^4 \ ^4\text{P} \longrightarrow 2p^3 \ ^4\text{S}^0$	NII	567.6–567.9	$3p \ ^3\text{D} \longrightarrow 3s \ ^3\text{P}^0$
			NII	424.2	$4f \ \text{F} \longrightarrow 3d \ ^3\text{D}^0$
			NII	399.5	$3p \ ^1\text{D} \longrightarrow 3s \ ^1\text{P}^0$
			NII	108.4–108.6	$2p^3 \ ^3\text{D}^0 \longrightarrow 2p^2 \ ^3\text{P}$

The helium atom lines wavelength and corresponding transitions are the following

Helium atom		
	Wavelength, $\lambda$ nm	Transition
HeI	667.8	$3d \ ^1\text{D} \longrightarrow 2p \ ^1\text{P}^0$
HeI	587.6	$3d \ ^3\text{D} \longrightarrow 2p \ ^3\text{P}^0$
HeI	492.2	$4d \ ^1\text{D} \longrightarrow 2p \ ^1\text{P}^0$
HeI	447.2	$4d \ ^3\text{D} \longrightarrow 2p \ ^3\text{P}^0$
HeI	388.9	$3p \ ^3\text{P}^0 \longrightarrow 2s \ ^3\text{S}$

### B. $\text{He}^+ - \text{O}_2$ collision system

$$\begin{aligned} \text{He}^+(1s) + \text{O}_2 &\longrightarrow \text{He}^* + \text{O}_2^+ \\ &\longrightarrow \text{He}^*(1s \ 2p) + \text{O}_2^+; \end{aligned} \quad (15)$$

$$\longrightarrow \text{He}^*(3p^3\text{P}_0) + \text{O}_2^+; \quad (16)$$

$$\text{and} \quad (17)$$

$$\begin{aligned} \text{He}^+(1s) + \text{O}_2 &\longrightarrow \text{He}(2s^2) + \text{O}_2^{+**} \\ &\longrightarrow \text{He}(2s^2) + \text{O}^*(3s' \ ^3\text{D}^0) + \text{O}^+(1s^2 2s^2 2p^3 \ ^4\text{S}_{3/2}^0); \end{aligned} \quad (18)$$

$$\longrightarrow \text{He}(2s^2) + \text{O}^*(4d \ ^3\text{D}^0) + \text{O}^+(2p^3 \ ^4\text{S}_{3/2}^0); \quad (19)$$

$$\longrightarrow \text{He}(2s^2) + \text{O}^*(3d^3 \ ^3\text{D}^0) + \text{O}^+(2p^3 \ ^4\text{S}_{3/2}^0); \quad (20)$$

$$\longrightarrow \text{He}(2s^2) + \text{O}^*(3s' \ ^1\text{D}^0) + \text{O}^+(2p^3 \ ^4\text{S}_{3/2}^0); \quad (21)$$

$$\longrightarrow \text{He}(2s^2) + \text{O}(1s^2 2s^2 2p^4 \ ^3\text{P}_2) + \text{O}^{+*}(1s^2 2s^2 2p^2 3d \ ^3\text{D}^0). \quad (22)$$

The wavelengths of the oxygen atom and ion, helium atom lines, and corresponding transitions are as follow:

Oxygen atom			Oxygen ion		
	Wavelength, $\lambda$ , nm	Transition		Wavelength, $\lambda$ , nm	Transition
OI	99.0	$3s' \ ^3D^0 \rightarrow 2p^4 \ ^3P$	OII	83.4	$2p^4 \ ^4P \rightarrow 2p^3 \ ^4S^0$
OI	97.4	$4d \ ^3D^0 \rightarrow 2p^4 \ ^3P$			
OI	102.6	$3d \ ^3D^0 \rightarrow 2p^4 \ ^3P$			
OI	115.2	$3s' \ ^1D^0 \rightarrow 2p^4 \ ^1D$			
Helium atom					
	Wavelength, $\lambda$ , nm	Transition		Wavelength, $\lambda$ , nm	Transition
HeI	53.7	$3p \ ^1P^0 \rightarrow 1s^2 \ ^1S$			
HeI	58.4	$2p \ ^1P^0 \rightarrow 1s^2 \ ^1S$			

### C. Experimental results and discussion

Figures 2a and 2b show the dependence of the emission spectra on the wavelength in the vacuum ultraviolet spectral range of 105 – 130 nm and visible spectral range of 490 – 580 nm, respectively, for collisions of  $E = 5$  keV helium ions with nitrogen molecules. Figure 2a presents the excitation spectra mostly for (with the exception of the ionic line  $\lambda = 108.4$  nm) nitrogen atomic lines, whereas Fig. 2b shows nitrogen ionic lines (with the exception of the atomic nitrogen line,  $\lambda = 493.5$  nm). The energy dependences of the excitation cross-sections for the same emission spectral lines are presented in Figs. 3a and 3b, respectively. The energy dependences of the helium atom emission cross-sections in the  $\text{He}^+ - \text{N}_2$  process on the energy of helium ions are shown in Fig. 3c. The results for the emission spectrum in the wavelength range of 80 – 105 nm in collisions of  $E = 10$  keV helium ions with oxygen molecules are presented in Fig. 4. The energy dependences of the emission cross-section for oxygen atomic OI (99.0, 102.6, 115.2, and 97.4 nm) and oxygen ionic OII (83.4 nm) lines in  $\text{He}^+ - \text{O}_2$  collisions are shown in Fig. 5a.

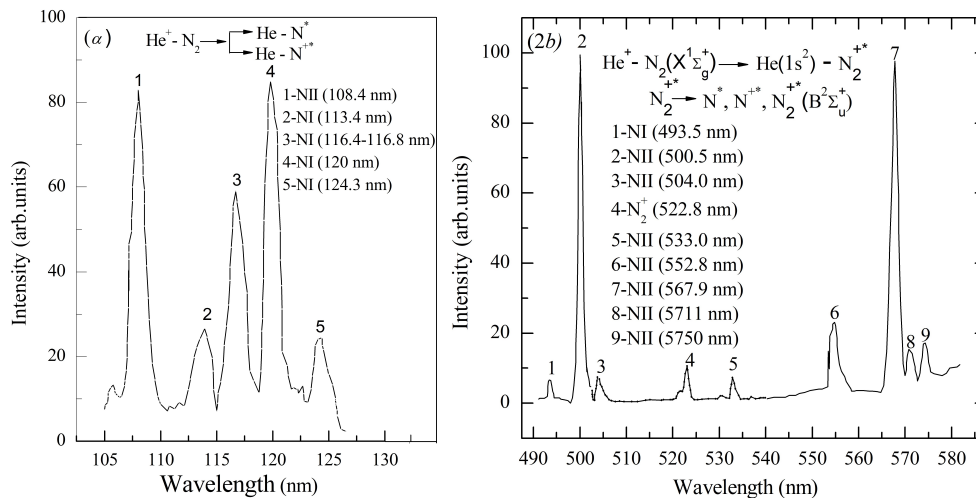


FIG. 2: (Color online) Dependence of the intensity on the wave length for  $\text{He}^+ \rightarrow \text{N}_2$  at (a) vacuum ultraviolet (80 – 130 nm) and (b) the visible (380 – 800 nm) spectral regions, respectively.

From the presented measurement results, special attention is given to the comparison of the energy dependence of helium atom excitation and nitrogen ion excitation. For this reason, we measure the excitation functions in visible spectral region for lines of helium atom HeI ( $\lambda = 388.9$  nm,  $3p \ ^3P \rightarrow 2s \ ^3S$ ) and nitrogen ion NII ( $\lambda = 500.1 - 500.5$  nm,  $3d \ ^3F \rightarrow 3p \ ^3D$ ) as well as polarization measurements for the same lines. The results of these measurements are shown in Figs. 6 and 7.

The analysis of the results shown in Figs. 2 and 4, as well as those shown in Figs. 3, 5, and 6, and polarization measurements presented in Fig. 7, allows us to draw some conclusion, related to the notable similarities of the processes considered in  $\text{He}^+ - \text{O}_2$  and  $\text{He}^+ - \text{N}_2$ , collision systems, and the electron-impact ionization in  $e - \text{N}_2$ ,  $e - \text{O}_2$  collision systems studied in [68].

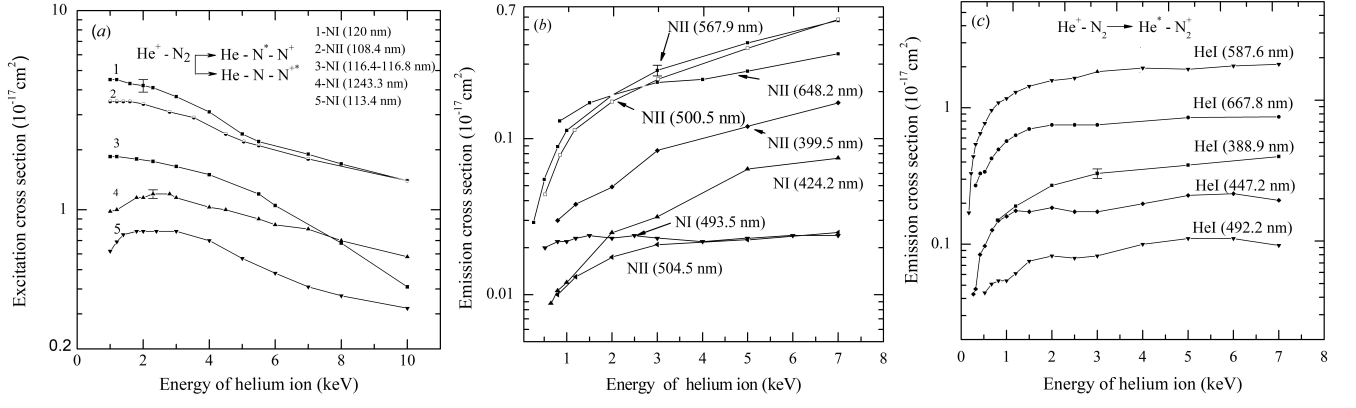


FIG. 3: (Color online) Energy dependence of the nitrogen atomic and ionic lines in the  $\text{He}^+ - \text{N}_2$  collision at (a) the vacuum ultraviolet and (b) the visible spectral regions, respectively. (c) Energy dependence of the helium atom emission cross sections in the process  $\text{He}^+ - \text{N}_2$  on the energy of helium ions.

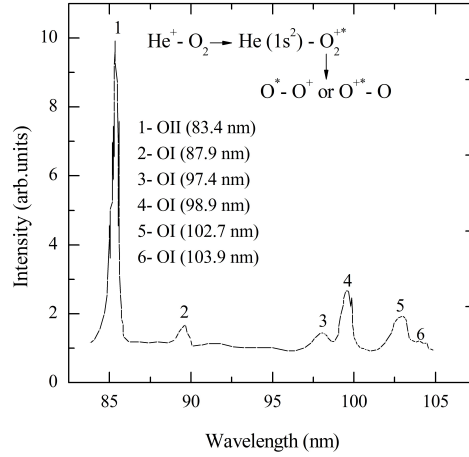


FIG. 4: (Color online) Emission spectrum in the wavelength range of 80 – 105 nm in collisions of 10 keV helium ions with oxygen molecules.

The striking similarities in  $\text{He}^+ - \text{O}_2$  and  $\text{He}^+ - \text{N}_2$  systems are as follow: i. the strong dominance of quasi-resonant charge-exchange processes; ii. the dominance of endothermic processes for similar energy defects; iii. population of exothermic channels, suggesting a strong dynamic effect. The dominance of electron-capture processes over direct – excitation processes, was also observed in [55]. In our case, most similarities related to the intensity of lines, energy dependences, and mechanisms in  $\text{He}^+ - \text{O}_2$  and  $\text{He}^+ - \text{N}_2$  collision systems are discussed in detail below.

Let us first consider the excitation processes of the dissociation products (nitrogen atoms and nitrogen ions) based on the results presented in Fig. 2 and 3.

In Fig. 2a, the curves corresponding to the two dominant atomic NI (120.0 nm,  $3s^4\text{P} \rightarrow 2p^3^4\text{S}$ ) and ionic NII (108.4 nm,  $2p^3^3\text{D} \rightarrow 2p^2^3\text{P}$ ) lines for the  $\text{He}^+ + \text{N}_2$  collision system exhibit a similar shape. Moreover, the absolute values of the excitation cross-sections for these lines are close to each other. These results suggest that the excitation mechanisms of the molecular states that dissociate into  $\text{N}^*(3s^4\text{P})$  and  $\text{N}^{+*}(2p^3^3\text{D})$  products are almost identical. In Ref. [55], the authors reached the same conclusion and showed that at relatively low energies,  $E \leq 3$  keV, charge exchange is the dominant process. According to this study, the  $1s$  vacancy of the  $\text{He}^+$  plays a determining role in different excitation processes. In the case of  $(\text{HeN}_2)^+$  ionic system, the initial vacancy in the He ( $1s$ ) orbital becomes an inner vacancy of the ionic atomic quasimolecule. Hence, core-excited molecular states were formed. The formation of excited products can be related to the decay of the intermediate molecular states of  $\text{N}_2^{+*}$ . Specifically, the molecular state that is correlated with either the  $\text{N}(3s^4\text{P}) + \text{N}^+(3\text{P})$  or the  $\text{N}(3s^2\text{P}) + \text{N}^+(^3\text{P})$  channels can be produced by the formation of a  $2s\sigma_g$  hole in the ground state of the  $\text{N}_2$  molecule [69].

Consequently, the emission of atomic NI (120.0 nm) and ionic NII (108.4 nm) nitrogen lines should be observed. Besides of these intense spectral lines, we observe also atomic NI (113.4 nm;  $2p^4^4\text{P} \rightarrow 2p^3^4\text{S}^0$ ) and ionic NII (91.6 nm;  $2s2p^3^3\text{P} \rightarrow 2p^2^3\text{P}$ ) and NII (77.6 nm;  $2s2p^3^1\text{D} \rightarrow 2p^2^1\text{D}$ ), which are not shown in Figs. 2a and 3a, and NII (108.4 nm;  $2p^3^3\text{D} \rightarrow 2p^3^3\text{P}$ ) lines (see spectral lines in Fig. 2a and energy dependences in Fig. 3a) that are formed

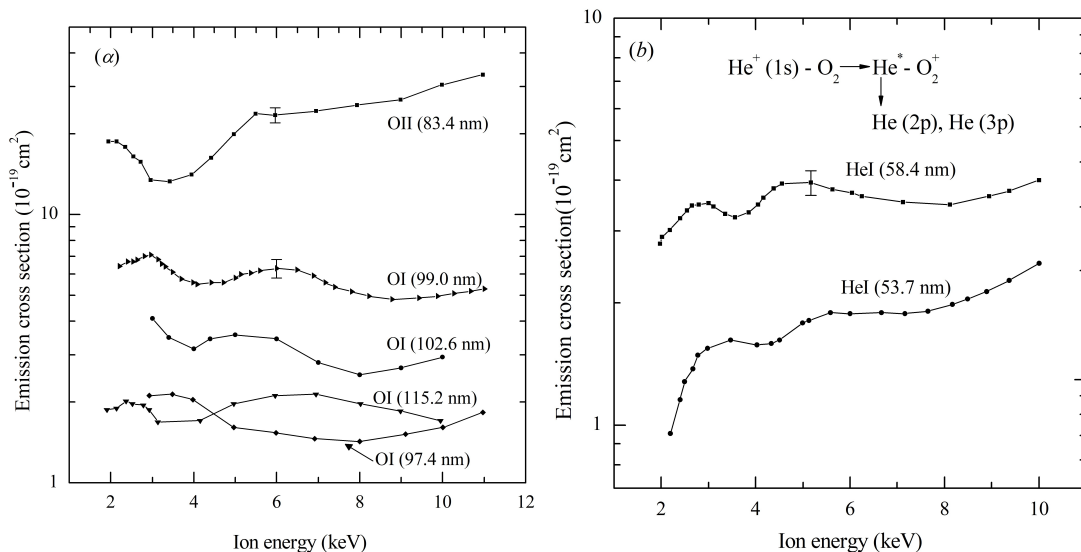


FIG. 5: (Color online) Energy dependences of the emission cross sections in  $\text{He}^+ - \text{O}_2$  collisions for (a) oxygen ionic OII (83.4 nm) and atomic OI (99.0, 102.6, 115.2, 97.4 nm) lines and (b) for HeI atomic (53.7, 58.4) lines.

by the removal of a  $2s$  electron from the inner electronic shell. The formation of these excited products can also be caused by the decay of core – excited molecular states. Unfortunately, not all molecular states that produce these lines during dissociation processes can be identified. Therefore, the formation of highly excited molecular states has received particular attention. These highly excited molecular states can be formed by the removal of a  $2s\sigma_g$  electron from the charge-exchange channel. To explain the excitation mechanism of this state, we used the schematic MO correlation diagrams for the  $(\text{HeN}_2)^+$  system from Ref. [61]. According to this diagram, when two partners approach each other one inner  $2\sigma_u$  electron fills the  $\text{He}(1s)$  vacancy, and the other  $3\sigma_g$  or  $1\pi_u$  electrons are promoted to a high Rydberg orbital. Hence, molecular states can be formed by using ionic cores. In these cases, a highly excited Rydberg orbital should produce molecular states of  $\text{N}_2^{+*}$  with  $^2\Sigma_g^+$  symmetry, which differ by two electrons from the  $\text{N}_2$  ground state [70]. It is also possible that the formation of excited atomic and ionic dissociation fragments can occur through decay of the  $^2\Sigma_g^+$  core-excited molecular Rydberg state.

The removal of the  $2s\sigma_g$  electron of the  $\text{N}_2$  molecule requires approximately 37 eV [69]. Therefore, excitation of the inelastic channel  $\text{He}(1s^2) + \text{N}_2^+(2\sigma_g^{-1})$  in the charge-exchange process (the ionization potential of He is 24.6 eV) is required to change the internal energy of the  $(\text{HeN}_2)^+$  system by approximately 12.4 eV. So, energy-loss spectra in the range  $10.5 < Q < 15.6$  eV observed in [55] in the charge exchange channel might contain this process.

Notable similarities in the energy dependences of the  $\text{He}^+ \rightarrow \text{N}_2$  collision system are observed in Fig. 3b. The energy dependences and absolute values of the cross-sections are the same for atomic ion lines of nitrogen NII (567.9 nm) with transition  $\text{N}^+(3p^3D \rightarrow \text{N}^+(3s^3P^0))$  and NII (500.5 nm) with transition  $\text{N}^+(2p3d^3F \rightarrow \text{N}^+(2p3p^3D))$ . The optical excitation functions of these two lines measured for the  $e - \text{N}_2$  collision system were studied in Ref. [71], where the term excitation function refers to the optical emission excitation function. The shapes of these two excitation functions (5680 Å and 5001 Å) in our study and [71] are virtually identical. The excitation of the relatively low-intensity atomic NI (113,4 nm,  $2p^4^4P \rightarrow 2p^3^4S$ ) and NI (124.3 nm  $3s^1^2D \rightarrow 2p^3^2D$ ) lines presented in Fig. 3a, can be associated with the direct one- and two-electron transitions due to the MO crossing, following MO promotion [71].

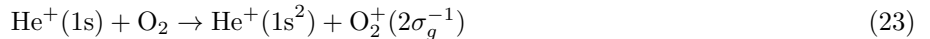
Proceeding in the same way as in the  $\text{He}^+ - \text{N}_2$  case, we measured the emission cross-section for the  $\text{He}^+ - \text{O}_2$  collision system. Figure 5a shows the energy dependence of the emission cross-section for the atomic OI (99.0, 102.0, 115.2, and 97.4 nm) and intense ionic OII (83.4 nm) oxygen lines. From these experimental data follows that the oxygen ion line OII (83.4 nm, the  $2p^4^4P \rightarrow 2p^3^4S_0$  transition) is the most intense for collisions with helium ions (Figs. 4 and 5a). The molecular dissociation that causes excited atomic and/or ionic fragments is due to the decay of a highly excited intermediate molecular state of the inner shell, where a collision-induced vacancy arises.

In the case of the  $\text{He}^+ - \text{O}_2$  collision, when the particles come closer together, a  $1s$  inner-shell vacancy of the helium atom turns into an inner-shell vacancy of a triatomic quasi-molecule. Accordingly, when the particles fall apart, an unstable and highly excited  $\text{O}_2^+$  molecular ion arises. Specifically, the decay of the  $2\sigma_g^{-1}$  vacancy in  $^2\Sigma_g^-$  and  $^4\Sigma_g^-$  highly excited molecular states leads to the formation of an excited dissociation product with the intense oxygen ion line OII (83.4 nm) [72].

An energy of approximately 46.2 eV is necessary to remove the  $2s\sigma_g$  electron from the inner shell of oxygen.

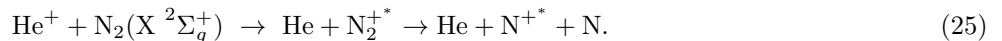


Therefore, the excitation of this inelastic channel during dissociative charge-exchange process



requires a change in the inner energy of the quasi-molecular system of  $(\text{He}, \text{O}_2)^+$  roughly by 22 eV. This estimate was indirectly confirmed in Ref. [73]. It appears that a broad peak in the energy loss spectrum near 22 eV, typical for charge-exchange, is related to this inelastic channel.

Let us now consider the similarities between the excitation of the He atom and the nitrogen ion lines. Experimental data for the excitation functions for the helium atom HeI ( $\lambda = 388.9$  nm,  $3p \ ^3P \rightarrow 2s \ ^3S$ ) and nitrogen ion NII ( $\lambda = 500.1 - 500.5$  nm,  $3d \ ^3F \rightarrow 3p \ ^3D$ ) lines are presented in Fig. 6. The curves exhibit surprising resemblance: in the entire investigated energy region, both the absolute values of the emission cross-sections and their energy dependence are close to each other. This behavior indicates the existence of a strong correlation between the dissociation products: the excited helium atoms and nitrogen ions



In addition, we assume that the inelastic energy defects for these channels are close to each other. Some additional arguments substantiate the existence of a correlation between channels (24) and (25). In Ref. [71] the electron-impact dissociative excitation of nitrogen molecules  $\text{N}_2$  was investigated. The authors observed the same emission line for  $\text{N}^+$ :  $\lambda = 500.5$  nm, corresponding to the transition  $3d \ ^3F \rightarrow 3p \ ^3D$ . Because the incident particle electron has a small mass, the experimentally obtained threshold energy of 57 eV, for the appearance of this line nearly coincides with the corresponding energy defect for this process. Therefore, for the threshold of 57 eV, after reduction by the ionization potential of the helium atom (24.6 eV), gives approximately 32 eV for the energy defect. In the energy loss spectrum plotted in [55], for the charge-exchange channel, one can find a broad peak in the vicinity of  $\sim 30$  eV. Thus, 32 eV is located in this area, which is indirect evidence in favor of the close relationship between reactions (24) and (25) [55].

#### D. Polarization

Let us consider the polarization following Ref. [74]. The polarization of the emission emerging from the excited  $^3P$ -state of helium is related to the relative populations of  $m_L = 0$  and  $m_L = \pm 1$  sublevels. The expression for the first Stokes' parameter is derived based on the general approach developed in [30]. The Appendix of Ref. [74] presents the details of these calculations, and the final formula for the linear polarization is as follows:

$$P = \frac{\mathcal{J}_{\parallel} - \mathcal{J}_{\perp}}{\mathcal{J}_{\parallel} + \mathcal{J}_{\perp}} = \frac{15(\sigma_0 - \sigma_1)}{41\sigma_0 + 67\sigma_1}, \quad (26)$$

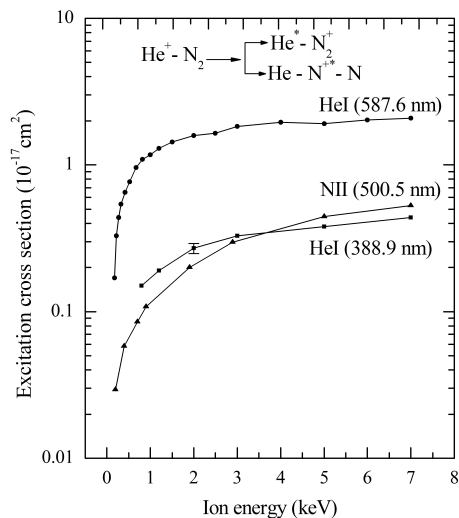


FIG. 6: (Color online) Energy dependence of the excitation cross section of helium atom and nitrogen ion lines: HeI (388.9 nm) and NII (500.5 nm).

where  $\mathcal{J}_{\parallel}$  and  $\mathcal{J}_{\perp}$  are the intensities of the radiation emitted in a direction perpendicular to the helium beam having electric vectors parallel and perpendicular to the beam direction, respectively. In Eq. (26),  $\sigma_0$  and  $\sigma_1$  represent cross-sections for the population of sublevels with  $m_L = 0$  and  $m_L = \pm 1$ , respectively. Our experimental observation leads to a value of  $P \sim 20\%$  in the energy range of 6.5 – 10 keV. From Eq. (26), we obtained the ratio  $\frac{\sigma_0}{\sigma_1} \approx 15$ . Such a large ratio value indicates that  $m_L = \pm 1$  sublevels of the excited helium atom are preferably populated. The latter implies that the electron density formed in the He\* during the collision is oriented perpendicularly with respect to the incident beam direction. In Fig. 7, the results of the polarization measurements are presented. The results indicate

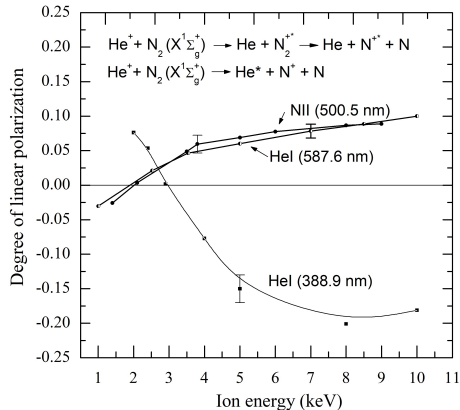


FIG. 7: (Color online) Energy dependence of the degree of polarization: HeI (388.9 nm), NII (500.5 nm), HeI (587.6 nm), our error bars represent one standard deviation.

the difference and similarities of polarization for the investigated emission lines. As shown, the maximum negative degree of polarization is 20% at the energy 8 keV for the HeI (388.9 nm) line, which is  $\sim 6\%$  for the NII (500.1 – 500.5 nm), which is a dissociation product. As shown in Fig. 7, the degrees of polarization for the HeI (587.6 nm) and NII (500.5 nm) emission lines change the sign at nearly the same energy  $\sim 2.3$  keV and appear to be independent of the He<sup>+</sup> incident energy in the range of 5 – 10 keV for the N<sup>+</sup> and 8 to 10 keV for He. A rise in polarization as the energy decreases was also noted for this transition in [75, 76]. They found that the polarization decreased to a value of approximately 5%. This result is consistent with our results. For the polarization of radiation emitted by the nitrogen ion N<sup>+</sup> (dissociation product) and helium atom He\*(3d <sup>3</sup>D) we use the same technique as in Ref. [74].

The energy dependence of the measured polarizations showed that the electronic orientation of the excited He atom changed at nearly 3 keV. It can be assumed that, because of the strong correlation between the excitation channels of He and N<sup>+</sup>, the electronic orientation of the excited nitrogen ion would also change. This implies that the effect of the molecular axis orientation with respect to the incident ion beam also changes as the energy increases.

#### IV. CONCLUSIONS

The striking similarities between the processes realized in the He<sup>+</sup>+N<sub>2</sub> and He<sup>+</sup>+O<sub>2</sub> collision systems have been reported. In collisions of helium ions with oxygen and nitrogen molecules, the intense atomic and ionic lines obtained are largely related to charge-exchange processes [10]. In both cases, the excited dissociative products (oxygen ion/atom and nitrogen ion/atom) are formed through the decay of the highly excited molecular states of the O<sub>2</sub><sup>+</sup>\* and N<sub>2</sub><sup>+</sup>\*, respectively.

We observed a similar shape of energy dependence, almost the same value of excitation cross-sections, as well as a common excitation mechanism for two dominant dissociative nitrogen atomic N\*(3s <sup>4</sup>P) and nitrogen ionic N<sup>+</sup>(2p<sup>3</sup> <sup>3</sup>D) products in the He<sup>+</sup>+N<sub>2</sub> collision. We found that these excited products could be formed by the removal of a 2s<sub>g</sub> electron in the charge-exchange channel. Notable similarities in the energy dependences and absolute values of the cross-sections for the nitrogen ionic lines NII (567.9 nm) and NII (500.5 nm) in He<sup>+</sup>+N<sub>2</sub> collisions were observed. The strong correlation between the excitation of the helium atomic HeI (388.9 nm, transition 3d <sup>3</sup>F → 3p <sup>3</sup>D) and the nitrogen ionic NII (500.1 – 500.5 nm, transition 3d <sup>3</sup>F → 3p <sup>3</sup>D) lines are revealed for the He<sup>+</sup>+N<sub>2</sub> collision system. The most intense oxygen ionic OII (83.4 nm) and atomic OI (99.0 nm) lines and weak (approximately 10<sup>-19</sup> cm<sup>2</sup>), double charged oxygen ion OIII (70.6 nm) lines were observed and identified in the collision of He<sup>+</sup> with O<sub>2</sub> molecules. In this case, the molecular dissociation that causes the excited atomic and/or ionic fragments is due to the decay of a highly excited intermediate molecular state of the inner shell, where a collision-induced vacancy arises. The highly excited molecular states (<sup>2</sup>Σ<sub>g</sub><sup>-</sup> and <sup>4</sup>Σ<sub>g</sub><sup>-</sup>) in He<sup>+</sup>+O<sub>2</sub> collisions are assigned, and their leading roles in explaining the

mechanism of the intense oxygen ionic OII (83.4 nm) and atomic OI (99.0 nm) lines are explained. Energy dependence of the degree of linear polarization for the He atomic lines HeI (388.9 nm and 587.6 nm) and nitrogen ionic line NII (500.5 nm) are measured. The maximum negative (20%) and minimum (5%) positive values of the degree of linear polarization are revealed for dissociative products of the helium atom (388.9 nm) and helium atom and nitrogen ion (587.6 nm; 500.1 nm), respectively, at the same collision energy  $E = 2.5$  keV. Based on polarization measurements, the cross-section  $\sigma_0$  and  $\sigma_1$ , related to the relative population of the helium He\* ( $^3P$ ) magnetic sublevels with  $m_L = 0$  and  $m_L = \pm 1$ , respectively, are calculated, and the ratio  $\sigma_1/\sigma_0 \approx 15$  is revealed. Such a high value of the ratio indicates that: i. the sublevels of the excited helium  $^3P$  state are preferably populated; ii. the electron density formed in the excited helium He\* atom during the collision was oriented perpendicular to the incident beam direction. Most of the experimental data obtained for the He<sup>+</sup>+N<sub>2</sub> and He<sup>+</sup>+O<sub>2</sub> collision systems were qualitatively interpreted in terms of quasi-diatomic approximation.

- 
- [1] M. R. Torr and D. G. Torr, The role of metastable species in the thermosphere. *Rev. Geophysics.* **20**, 91 (1982).  
 [2] T. E. Cravens et al., Energetic ion precipitation at Titan. *Geophysics. Res. Lett.* **35**, L03103 (2008).  
 [3] Pararicas, C., Mauk, b.H., Ratliff, J.M., Cohen, C., and Johnson, R.E., *Geophysics. Res. Lett.*, **29**, 18, (2002).  
 [4] H. Luna et al., *Astrophys J.* **628**, 1086 (2005).  
 [5] R. K. Janev Atomic and Molecular Processes in Fusion Edge Plasmas, Plenum Press, New York, 1995.  
 [6] S. E. Huber, A. Mauracher, D. S.ub, I. Sukuba, J. Urban, D. Boyrodin, and M. Probst, *J. Chem. Phys.* **150**, 024306 (2019).  
 [7] R. Ya. Kezerashvili and G. L. Matloff, *Adv. Space Res.* **44**, 859 (2009).  
 [8] L. Campbell, M.J. Brunger, P.J. Teubner, D.C. Cartwright, *J. Electron Spec. and Related Phenomena* **144**, 119 (2005).  
 [9] K. J. Remick, R. K. Smith, D. Lummerzheim, *J. Atmospheric, Solar-Terrest. Phys.* **63**, 295 (2001).  
 [10] A. Shinsuke, N. Ebizuka, et al. *Astrophys. J.* **618**, L141 (2005).  
 [11] P. Jenniskens, C. O. Laux, and E. L. Schalle, *Astrobiology* **4**, 109 (2004).  
 [12] D. E. Shemansky and X. Liu, *J. Geophys. Res.*, **110**, A07307 (2005).  
 [13] A.W. Harrison, and A. Vallance Jones, *J. Atmospheric Terrestrial Phys.* **13**, 291 (1959).  
 [14] M. Hollstein, D. C. Lorents, J. R. Peterson, and J. R. She Ridan, *Can. J. Chem.* **47**, 1858 (1969).  
 [15] D. E. Shemansky and A. L. Broadfoot, *J. Quant. Spectrosc. Radiat. Transfer*, **11**, 1385 (1971).  
 [16] L.G. Piper, B.D. Green, W.A. Lumbergand, S.J. Wolnik, *J. Phys. B: At. Mol. Phys.* **19**, 3327 (1986).  
 [17] R.L. Gattinger and A. Vallance Jones, *Can. J. Phys.* **52**, 2343 (1974); *Can. J. Phys.* **59**, 480 (1981).  
 [18] L. Campbell, D. C. Cartwright, M. J. Brunger, and P. J. O. Teubner, *J. Geophys. Res.* **111**, A09317 (2006).  
 [19] O. Yenen, D. H. Jaecks, and R. I. Martin, *Phys. Rev. A* **35**, 1517 (1987).  
 [20] P. Baltzer, W. Wannberg, L. Karlsson, et al., *Phys. Rev. A* **45**, 4374 (1992).  
 [21] A. V. Golovin, F. Heiser, C. J. K. Quayle, et al., *Phys. Rev. Lett.* **79**, 4554 (1997).  
 [22] P Erman, A. Karawajczyk, E. Rachlew-Kallne, et al., *J. Phys. B* **29**, 5785 (1996).  
 [23] P. Erman, A. Karawajczyk, E. Rachlew-Kallne, et al., *Phys. Scr.* **49**, 308 (1994).  
 [24] D. M. P. Holland, D. A. Shaw, S. M. McSweeney, et al., *Chem. Phys.* **173**, 315 (1993).  
 [25] M. Kato, K. Kameta, T. Odagiri, et al., *J. Phys. B* **35**, 4383 (2002).  
 [26] M. Kato, T. Odagiri, K. Kameta, et al., *J. Phys. B* **36**, 3541 (2003).  
 [27] M. Ukai, S. Machida, K. Kameta, et al., *Phys. Rev. Lett.* **74**, 239 (1995).  
 [28] A. A. Cafolla, T. Reddish, and J. Comer, *J. Phys. B* **22**, L273 (1989).  
 [29] H. Liebel, A. Ehresmann, H. Schmoranzner, et al., *J. Phys. B* **35**, 895 (2002).  
 [30] J. H. Macek and D. H. Jaecks, *Phys. Rev. A* **4** 2288, (1971).  
 [31] U. Fano and J. H. Macek, *Rev. Mod. Phys.* **45**, 553 (1973).  
 [32] I. C. Malcolm, H. W. Dassen, and J. W. McConkey, *J. Phys. B: Atom. Molec. Phys.* **12**, 1003 (1979).  
 [33] D. H. Jaecks, O. Yenen, M. Nataragan, and D. Mueller, *Phys. Rev. Lett.* **50** 825 (1983).  
 [34] R. Hippler, M. Faust, R. Wolf, H. Kleinpoppen, and H. O. Lutz, *Phys. Rev. A* **31**, 1399 (1985).  
 [35] R. Hippler, M. Faust, R. Wolf, H. Kleinpoppen, and H. O. Lutz, *Phys. Rev. A* **36**, 4644 (1987).  
 [36] O. Yenen and D. H. Jaecks, *Phys. Rev. A* **32**, 836, (1985).  
 [37] O. Yenen, D. H. Jaecks, and P. J. Martin, *Phys. Rev. A* **35**, 1517 (1987).  
 [38] C. Richter, D. Dowk, and J. C. Houver, *J. Phys. B: At. Mol. Opt. Phys.* **24**, L213 (1991).  
 [39] R. Hippler, *Phys. B At. Mol. Opt. Phys.* **26**, 1 (1993).  
 [40] B. Siegmann, R. Hippler, and H. O. Lutz, *J. Phys. B: At. Mol. Opt. Phys.* **31**, L675 (1998).  
 [41] H. Tanuma, T. Hayakawa, C. Verzani, and H. Kano, H Watanabe, B. D. DePaola, and N Kobayashi, *J. Phys. B: At. Mol. Opt. Phys.* **33**, 5091 (2000).  
 [42] H. Merabet, R. Bruch, S. Fulling, K. Bartschat, and A. L. Godunov, *J. Phys. B: At. Mol. Opt. Phys.* **36**, 3383 (2003).  
 [43] E. Stambulchik and Y. Maron, *Phys. Rev. A*, **65**, 052726 (2002).  
 [44] J. R. Oppenheimer, *Z. Phys.* **43**, 27 (1927).  
 [45] I. C. Percival and M. J. Seaton, *Philos. Trans. R. Soc. London Ser. A* **251**,113 (1958).

- [46] E. Takacs, E. S. Mheyer, J. D. Gillaspay, et al., Phys. Rev. A, **54**, Number 2, August (1996).
- [47] D. W. O. Heddle and R. G. W. Keesing – Proc. Royal Soc. London. Series A, Math. and Phys. Sciences, **299**, No. 1457 (Jun.14, 1967)212, (1967).
- [48] A. L. Godunov, H. Merabet, J. H McGuire, R. Bruch, J. Hanni, and V. S. Schipakov, J. Phys. B: At. Mol. Opt. Phys. **34**, 2575 (2001).
- [49] A. L. Godunov, P. B. Ivanov, V. A. Schipakov, P. Moretto-Capelle, D. Bordenave-Montesquieu, and A. Bourdenave-Montesquieu, J. Phys. B: At. Mol. Opt. Phys. **33**, 971 (2000).
- [50] K. Blum, Density Matrix. Theory and Applications, New York, Plenum, 1981.
- [51] J. Watson and R. J. Anderson, J. Chem. Phys. **66**, 4025 (1977).
- [52] R. J. Van Brunt and R. N. Zare, J. Chem. Phys. **48**, 4304 (1968 ).
- [53] A. R. Filippelli, F. A. Sharpton, and C. C. Lin, J. Chem. Phys. **76**, 3597 (1982).
- [54] R. J. Van Brunt and R. N. Zare, J. Chem. Phys. **48**, Number 9, 1 May (1968).
- [55] D. Doweck, D. Dhuicq, J. Pommier, et al., Phys. Rev. A **24**, 2425 (1981).
- [56] F. B. Yousif, B. G. Lindsay, F. R. Simpson, and C. I. Latimer, J. Phys. B; At. Mol. Phys. **20**, 5079 (1987).
- [57] D. Doweck, D. Dhuicq, V. Sidis, and M. Barat, Phys. Rev. A **26**, 746 (1982).
- [58] D. P. De Bruijn, J. Neuteboom, and J. Loss, Chem. Phys. **85**, 233 (1984).
- [59] I. Kuen, H. Story, and F. Howorka, Phys. Rev. A **28** 119 (1983).
- [60] M. R. Gochitashvili, V. A. Ankudinov, V. M. Lavrov, and B. I. Kikiani, Zh. Tech. Fiz. **49**, 2338 (1979); [Soviet Tech. Phys. **24**, 1303 (1979)].
- [61] D. Doweck, D. Dhuicq, and M. Barat, Phys. Rev. A **28**, 2838 (1983).
- [62] M, R. Gochitashvili, R. Ya. Kezerashvili, and R. A. Lomsadze, Phys. Rev. A **82**, 022702 (2010)
- [63] R. A. Lomsadze, M. R. Gochitashvili, R. Ya. Kezerashvili, N. O. Mosulishvili, and R. Phaneuf, Phys. Rev. A, **87**, 042710 (2013).
- [64] M. R. Gochitashvili, R. V. Kvidzhinadze, N. R. Djaliashvili, and B. I. Kikiani, Thechnical Physics **38**, 851 (1993).
- [65] V. V. Skubenich, I. P. Zapesochni, Geomagnetizm and Aeronomia **21**, 481. (1981).
- [66] W. R. Pendleton, R. R. O’Neil, J. Chem. Phys. **56**, 6260 (1972).
- [67] D. C. Cartwright, J. Chem. Phys. **58**, 178 (1973).
- [68] R. A. Lomsadze, M. R. Gochitashvili, R. Ya. Kezerashviliy, and M. Schulz, Int. J. Mod. Phys. B **35**, 2150104 (2021).
- [69] K. C. Smyth, J. A. Schiavone, and R. Freund, J. Chem. Phys. **59**, 5225 (1973).
- [70] H. Sambe and D. E. Ramaker, Chem. Phys. **107**, 351 (1986).
- [71] A. R. Filippelli, F. A. Sharpton, C. C. Lin, and R. E. Murphy, J. Chem. Phys. **76**, 3597 (1982).
- [72] R. S. Freund, J. Chem. Phys. **54**, 3125 (1971).
- [73] Table of Molecules, National Institute of Standards and Technology, 2000.
- [74] M. Gochitashvili, I. Noselidze, T. Chighvinadze, R. Lomsadze, Polarization measurements in  $\text{He}^+ - \text{N}_2$  collisions. Georgian Elect. Sci. J.: Physics **1** (39-2) (2004).
- [75] W. E. Lamb and T. H. Maiman, Phys. Rev. **105**, 573 (1957).
- [76] R. H. Hughes, R. B. Kay, and L. D. Weaver, Phys. Rev. **129**, 1630 (1963).